Comments on "A Multiscale Numerical Study of Hurricane Andrew (1992). Part I: Explicit Simulation and Verification"

MARK D. POWELL AND SAMUEL H. HOUSTON

NOAA/Hurricane Research Division, Miami, Florida

1. Introduction

In their paper "A multiscale numerical study of Hurricane Andrew (1992). Part I: Explicit simulation and verification," Liu et al. (1997, hereafter referred to as LZY) present an impressive simulation of a mature tropical cyclone initialized with environmental data and operational model analyses obtained during Hurricane Andrew. The simulated tropical cyclone makes landfall near Palm Beach, Florida, with an eye diameter about twice that observed. The minimum central sea level pressure at landfall is similar to that observed when Hurricane Andrew made landfall about 105 km farther south near Homestead, Florida. According to Fig. 2 of LZY, the simulated storm begins filling at landfall and its pressure increases to about 944 hPa in 5 h, similar to that observed in Andrew (Powell et al. 1996; Powell and Houston 1996, hereafter referred to as PHR and PH). LZY compared the surface wind field of the simulated storm to that observed in Hurricane Andrew by PH and suggested that the coastal discontinuities published in PH were the product of reducing flight-level winds to the surface with a planetary boundary layer (PBL) model, analyzing land and marine observations separately, and then merging them at the coastline "without including full dynamic and physics interactions." LZY provided little information on the prelandfall wind distribution and land surface properties to substantiate the landfall wind field produced by their model. The reply to this comment (Zhang et al. 1999, hereafter referred to as ZLY) indicates that the landfall winds described in LZY correspond to a completely different framework for exposure, height, and averaging time than that used by PH. The lack of coastal discontinuities in LZY's landfall wind field corresponds to a distinct prelandfall wind distribution that differs both from the observations and earlier hours of the simulation.

Corresponding author address: Dr. Mark D. Powell, NOAA-HRD-AOML, 4301 Rickenbacker Cswy., Miami, FL 33149.
E-mail: powell@aoml.noaa.gov

The purpose of this comment is to discuss differences between the observed (PH) and simulated (LZY) surface wind distributions at landfall and to compare the modeled and observed wind maxima using a standard framework.

2. Distribution of surface winds at landfall

The only prelandfall simulated wind fields shown by LZY (in their Fig. 16, valid for 2000 UTC 23 August, about 11 h before simulated landfall) show a wind maximum in the northern semicircle at the 95.0- and 85.0-kPa levels. The LZY landfall wind field (Fig. 7 of LZY) contained maximum winds on the north side of the storm with maximum winds over land of about the same magnitude as adjacent winds over the water with little indication of a discontinuity associated with the land–sea roughness change. While location of the wind maximum on the north side compared well with the observed wind field described in PH, the lack of any discontinuity along the coastline was suspect. Coastal wind discontinuities have been observed in numerous storms (Graham and Hudson 1960)—the Lake Okeechobee hurricanes of 1949 and 1950 (Myers 1954), Hurricanes Belle of 1976 (SethuRaman 1979), Frederic of 1979 (Powell 1982), Alicia of 1983 (Powell 1987), Hugo of 1989 (Powell et al. 1991), and Andrew (PHR; PH)—as well as in numerical simulations of tropical cyclone landfall wind fields (Moss and Jones 1978; Tuleya and Kurihara 1978; Tuleya et al. 1984; Tuleya 1994). As described in PH (section 3a), this discontinuity actually corresponds to a transition zone where the flow is in the process of adjusting to a new underlying surface.

In their reply, Fig. 3c of ZLY describes the simulated wind field 2 h prior to landfall showing strongest winds in a semicircle on the *west* (landward) side of the storm at 40 m. The landward wind maxima is quite different from the northward maximum described 11 h earlier in LZY (Fig. 16) and helps explain the lack of a coastal wind discontinuity. With this type of maximum wind distribution the frictional effects at landfall would reduce the west semicircle wind maximum such that the

A

92082211: ANDREW
Total Wind Speed   XY Slice at 0.5 km

23:53:00 to 24:36:30 UTC

B
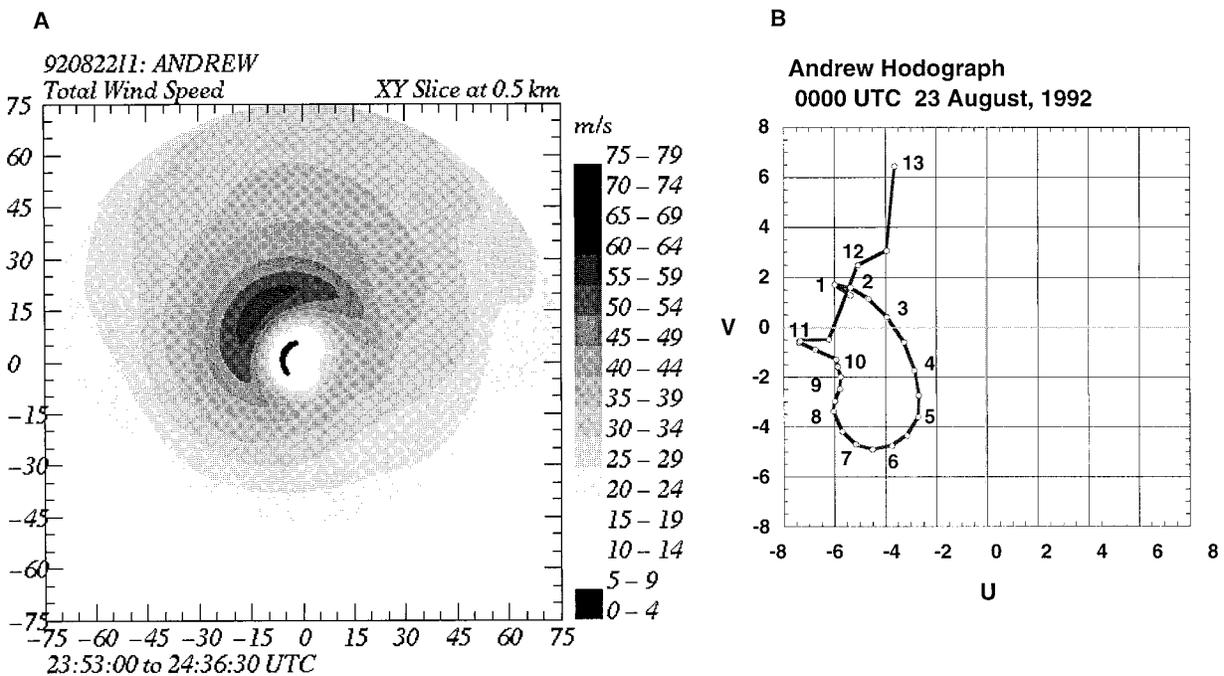
**Andrew Hodograph
0000 UTC 23 August, 1992**

FIG. 1. (a) Hurricane Andrew wind speed distribution for 0000 UTC 23 August 1992 at the 0.5-km level derived from NOAA P3 airborne Doppler radar wind measurements using the extended velocity track display method. (b) Hodograph created from Doppler wind measurements using EVTD. East–west (U) and north–south (V) component winds in m s^{-1}, numbers adjacent to curve mark altitudes in km.

differences between maximum winds over land and water would be small. Effectively, this results in a rotation of the wind maximum to just offshore on the north side (Fig. 4a of ZLY). The LZY simulation is remarkably similar to a study by Moss and Jones (1978) for a hurricane moving west at 5 m s^{-1}. In their simulation, a low-level wind maximum initially in the right (north) semicircle rotated to the landward side several hours before landfall with a subsequent shift of the maximum winds to the north side at landfall. A simulation for a storm moving west at 10 m s^{-1} by Tuleya et al. (1984) maintained maximum surface winds in the northern semicircle throughout the landfall process. For translation speeds similar to Andrew, tropical cyclone boundary layer flow models (Myers and Malkin 1961; Shapiro 1983; Wang and Holland 1997) suggest a wind maximum on the front right or right side of the storm (relative to the earth), but do not address landfall.

The physical processes associated with a shift of the simulation wind maximum to the landward front (west) semicircle shortly before landfall are of great interest since the northwesterly flow over land obstacles on the west side would contain much higher turbulent intensity than northeasterly flow with a marine fetch on the north side. An investigation relating landfall wind distribution changes to variations in model parameters, storm speed, and environmental flow specifications would help to understand the model's sensitivity and suggest processes that may be important at landfall.

At ~0000 UTC 23 August, while Andrew was in its

deepening stage at 96.0 kPa, the National Oceanic and Atmospheric Administration (NOAA) P3 research aircraft were conducting a synoptic flow experiment and collected wind velocity measurements with the airborne Doppler radar. Using the extended velocity track display (EVTD) method (Roux and Marks 1996), the wind distribution at 500 m (Fig. 1a) depicts maximum wind speeds on the northwestern side that persisted through 5 km.

A persistent shift in the azimuthal position of the wind maximum with height could be produced by vertical shear of the environmental flow (Marks et al. 1992). A front-side, landward wind maximum at the surface implies a strong cross-track environmental shear associated with northerly flow at the surface. A hodograph created from the EVTD analysis (Fig. 1b) shows very little cross-track shear in the lower 3 km. Northerly shear is suggested from 3 to 6 km, with southerly shear from 8 to 13 km.

Examination of air force reconnaissance eyewall passes at 3 km from 23 August (not shown) confirm that the wind maximum was maintained in the right (north) semicircle for the entire prelandfall period. Highest winds were located 16–25 km north (~0330 UTC), northwest (~1200 UTC), and northeast (~1600–2230 UTC) of the center on 23 August and then remained north of the center through landfall. Considering that the position of the wind maxima at the 500-m and 3.0-km levels were well correlated from the earlier Doppler measurements, a landward shift of the surface

wind maximum to the front semicircle is not consistent with the observations.

A large convective asymmetry could influence the azimuthal position of the maximum surface winds as indicated in Hurricane Emily of 1993 (Burpee et al. 1994). Since Miami WSR-57 radar observations of Andrew's eyewall (see Wakimoto and Black 1994) indicated a symmetric ring of convection at low levels about 30 min before landfall, there is little evidence that the wind maximum at lower levels shifted to the front (west) semicircle just before landfall due to a convective asymmetry. Convective asymmetries were observed during and after landfall. Willoughby and Black (1996) used radar reflectivity measurements at the 3–8-km level from the Tampa WSR-57 to describe a process of cell development initiated where easterly flow associated with the north side wind maximum in the eyewall impinged on the coast, creating reflectivity maxima on the west and southwest sides of the storm, but this process was not supported by Melbourne WSR-88D radar measurements discussed in PH.

It is possible that stronger winds were present below the 3-km flight level as discussed in PHR. Safety considerations in mature hurricanes often preclude reconnaissance flights at the levels most likely to contain the strongest winds (Powell and Black 1990). Accordingly, for adjustment to the surface, PHR used the peak 10-s flight-level observations in the vicinity of the eyewall, noting the tendency for convection to vertically distribute the wind maximum in strong, mature hurricanes. As discussed in PHR (section 5) the analysis of Andrew's wind field at landfall is not totally dependent on adjusted flight-level winds. The northwest quadrant of the eyewall was represented by Fowey Rocks C-MAN station, the north part of the eyewall contained the highest wind measurement obtained in Andrew (by a Perrine homeowner), and the maximum winds in the southwestern and southeastern sides of the eyewall were observed by an instrument aboard a moored sailboat. In these critical locations, surface observations are well represented by the PH analysis. Although it is possible that slightly higher winds may have occurred after the final observations at Fowey and Perrine on the northwest and north sides of the eyewall, and that stronger winds may have been present in data voids on the west side, the observations compared well with nearby adjusted flight-level winds and were consistent with the location of the maximum radar reflectivity in the eyewall. The PH depiction of the maximum sustained surface winds on the north side of the eyewall is also consistent with the distribution of F2 damage from independent storm debris surveys by Fujita (1992) and Wakimoto and Black (1994). Locations containing the largest insurance losses and electrical utility damage also correlate with a north eyewall wind maximum but relatively high damage was spread throughout the entire area affected by the eyewall due to duration and wind direction steadiness effects described by Powell et al. (1995).

3. Comparison of maximum winds using a standard framework

Hurricane surface winds are strongly dependent on the averaging time attributed to the wind observations, the roughness of the underlying surface, and height of the wind measurements. The identification of wind speed averaging times, heights, and local terrain is critical in the comparison of observed wind speeds to those obtained from numerical models. PHR documented the assembly and quality control of all available surface and flight-level wind measurements collected in south Florida during Hurricane Andrew, adjusting the land observations to a common "open terrain" exposure at 10-m level with an averaging time corresponding to the maximum 1-min sustained surface wind that might occur over some longer period. In their reply, ZLY provide details on model grid cell wind exposure (specified by land use/land cover over land or defined by a roughness length parameterization over the sea), averaging time (a 13-s time step) and height (40 m) over the ocean or land. While these data help to explain the simulated wind field, the model wind field represents a completely different framework than that used by PH.

a. Standard framework for surface winds in hurricanes

The National Hurricane Center (NHC) issues hurricane warnings and advisories using the term "maximum sustained surface wind." This wind is defined as the maximum 1-min wind that might be observed at a height of 10 m over open terrain exposure over land. PHR described how to standardize wind observations to this common framework. To be truly comparable, models should attempt to output surface wind fields in this framework. Fortunately, since most models rely on surface layer similarity, it is a straightforward matter to compute a 10-m wind field for open terrain and then use a 1-min gust factor to compute the highest 1-min wind over the timescale corresponding to the model grid cell.

b. Adjustment to standard height and exposure

According to ZLY, the "surface wind" described by the model actually corresponds to a surface layer mean at 40 m. Although the contour interval of Fig. 2 of ZLY suggests little difference between land and marine winds, the friction velocities and roughness actually correspond to significant differences of over 10 m s^{-1}. With a typical strong-wind, neutral-stability logarithmic surface layer [Eq. (2) of PHR], 40-m-level winds of 57 m s^{-1} (based on a friction velocity of 4.3 m s^{-1} from Fig. 2 of ZLY) would decrease to 42 m s^{-1} at the 10-m level over the marsh or wetland terrain (0.2-m roughness length) corresponding to the simulation's strongest overland winds. Maximum marine winds of 69 m s^{-1} [based on a friction velocity of 4.3 m s^{-1} and roughness of

TABLE 1. Comparison of simulated and observed landfall wind maxima.

Exposure	LZY framework		NHC–PHR framework	
	Land	Sea*	Land	Sea**
Roughness (m)	0.20	0.06	0.03	0.017
Friction velocity (m s^{-1})	4.3	4.3	3.76	3.89
Model 40 m (m s^{-1})	56.9	69.8	67.6	76.7
Model 10 m (m s^{-1})	42.1	54.9	54.6	63.2
Model 10 m (m s^{-1}) adjusted to max 1-min wind	46.3	60.4	60.0	69.5
Observed 10 m (m s^{-1}) (PH, max 1 min)	—	—	62.0	66.0

* Computed from Charnock's relationship using $\alpha = 0.032$ (ZLY).
** Computed from Charnock's relationship using $\alpha = 0.011$.

0.06 m from Fig. 2 and Eq. (4) of ZLY] reduce to 55 m s^{-1} at 10 m.

In reality, the region attributed to marsh or wetland comprises a population and infrastructure for over two million people; LZY may wish to consider using a higher-resolution land use/land cover database for future simulations. The marine roughness lengths described by the Charnock relationship [Eq. (4)] of ZLY [also used in Geophysical Fluid Dynamics Laboratory (GFDL) model landfall simulations by Tuleya et al. (1984)] date back to work published in the 1960s and are much larger than those in the more recent literature (e.g., Garratt 1977; Wu 1982). Since the roughness lengths used in ZLY are roughly a factor of 3 larger than PHR in the region of maximum marine winds (e.g., 0.06 m vs 0.017 m), the simulated marine winds (and land–sea differences) would be larger if LZY used a smaller Charnock constant (α) in line with more recent literature (e.g., $\alpha = 0.011$ to 0.018). The GFDL modelers have since recognized this and changed their Charnock constant to $\alpha = 0.0185$ (Bender et al. 1993). We should note, however, that much work remains to parameterize sea surface roughness in terms of wave age and surface stress (Donelan 1993). Using Eq. (3) of PHR, maximum 10-m-level marine winds would increase from 55 to 63 m s^{-1} using a 0.015-m roughness length and $\alpha = 0.011$.

If we convert the land exposure used in the simulation to the same framework used by PH (Table 1), using Eq. (3) of PHR, maximum 10-m winds for open terrain over land increase to 54.6 m s^{-1}, reducing the land–sea wind speed differences (since the 0.03-m open terrain roughness is only slightly larger than over water).

c. Adjustment to maximum sustained wind and comparison to observed maxima

To complete the conversion to the standard framework we need to address the timescale of the grid cell and compute the highest 1-min wind that might have occurred during that time period. It is not clear what time period a 13-s model time step might correspond to over a 6-km grid cell, but since similarity theory used in the simu-

lation is only valid for long time averages it should be at least be representative of something on the order of 10 min or more (PHR use 10 min as the timescale of the PBL-model-adjusted aircraft measurements). Hence, using the 1-min gust factor relationship shown in Fig. 9 of PHR, simulation winds would need to be increased on the order of 10% to be comparable to a maximum 1-min wind that might occur over the grid cell. Using the same framework employed by NHC and PH for comparison, the maximum 1-min sustained simulated winds for open terrain at 10 m (Table 1) are 60 m s^{-1} over land and 69.5 m s^{-1} over water (using 0.015-m roughness), within 5% of the observationally based PH winds of 62 m s^{-1} over land and 66 m s^{-1} over water.

Please note we are not suggesting that models use open terrain roughness everywhere over land for time step calculations; the standard framework discussed above is a useful diagnostic field providing a conservative estimate or upper bound on the maximum sustained surface winds and allows models and observations to be compared on even terms.

4. Conclusions

LZY appear to have been successful in simulating much of the overall behavior of a mature tropical cyclone landfall. While very similar to results obtained by Moss and Jones (1978), LZY's placement of the model wind maximum in the front landward semicircle just before landfall is not consistent with the measurements of maximum winds in the right northern semicircle or more recent GFDL model simulation studies. Analyses of surface winds fields in Atlantic hurricanes since 1993 (see the storms atlas at http://www.aoml.noaa.gov/hrd) show no examples of a persistent shift in the wind maximum to the landward front semicircle for storms approaching landfall. However, unusual wind asymmetries (e.g., wind maximum on the left or left front side) have been observed near landfall in slow-moving storms with asymmetric convection (e.g., Hurricanes Emily of 1993 and Danny of 1997). We encourage LZY to conduct additional landfall experiments to investigate the sensitivity of the surface wind field to variations in model parameters and environmental conditions.

When compared in a standard framework, the magnitude of LZY's model wind maxima at landfall compares favorably with observations. Since most models rely on surface layer similarity theory, it should be straightforward to compute a 10-m-level wind field consistent with the framework used by the National Hurricane Center and PHR. We invite future comparisons of surface wind field simulations to recently observed hurricanes using the standard framework.

ments. Reviews of the manuscript by Peter Black, Frank Marks, and Peter Dodge are appreciated.

REFERENCES

Bender, M. A., I. Ginis, and Y. Kurihara, 1993: Numerical simulations of tropical cyclone—Ocean interaction with a high-resolution coupled model. *J. Geophys. Res.,* **98,** 23 245–23 263.

Burpee, R. W., and Coauthors, 1994: Real-time guidance provided by NOAA's Hurricane Research Division to forecasters during Emily of 1993. *Bull. Amer. Meteor. Soc.,* **75,** 1765–1783.

Donelan, M. A., F. W. Dobson, S. D. Smith, and R. J. Anderson, 1993: On the dependence of sea surface roughness on wave development. *J. Phys. Oceanogr.,* **23,** 2143–2149.

Fujita, T. T., 1992: Damage survey of Hurricane Andrew in south Florida. *Storm Data,* Vol. 34, NCDC, 25–30.

Garratt, J. R., 1977: Review of drag coefficients over oceans and continents. *Mon. Wea. Rev.,* **105,** 915–929.

Graham, H. E., and G. N. Hudson, 1960: Surface winds near the center of hurricanes (and other cyclones). NHRP Rep. 39, 200 pp. [Available from NOAA Library, 4301 Rickenbacker Cswy., Miami, FL 33149.]

Liu, Y., D. Zhang, and M. K. Yau, 1997: A multiscale numerical study of Hurricane Andrew (1992). Part I: Explicit simulation and verification. *Mon. Wea. Rev.,* **125,** 3073–3093.

Marks, F. D., Jr., R. A. Houze Jr., and J. F. Gamache, 1992: Dual-aircraft investigation of the inner core of Hurricane Norbert. Part I: Kinematic structure. *J. Atmos. Sci.,* **49,** 919–942.

Moss, M. S., and R. W. Jones, 1978: A numerical simulation of hurricane landfall. NOAA Tech. Memo. ERL NHEML-3, 15 pp. [Available from NOAA Library, 4301 Rickenbacker Cswy., Miami, FL 33149.]

Myers, V. A., 1954: Surface friction in a hurricane. *Mon. Wea. Rev.,* **82,** 307–311.

——, and W. Malkin, 1961: Some properties of hurricane wind fields as deduced from trajectories. NHRP Rep. 49, 45 pp. [Available from NOAA Library, 4301 Rickenbacker Cswy., Miami, FL 33149.]

Powell, M. D., 1982: The transition of the Hurricane Frederic boundary layer wind field from the open Gulf of Mexico to landfall. *Mon. Wea. Rev.,* **110,** 1912–1932.

——, 1987: Changes in the low-level kinematic and thermodynamic structure of Hurricane Alicia (1983) at landfall. *Mon. Wea. Rev.,* **115,** 75–99.

——, and P. G. Black, 1990: The relationship of hurricane reconnaissance flight-level wind measurements to winds measured by NOAA's oceanic platforms. *J. Wind Engineer. Indust. Aerodyn.,* **36,** 381–392.

——, and S. H. Houston, 1996: Hurricane Andrew's landfall in South Florida. Part II: Surface wind fields and potential real-time applications. *Wea. Forecasting,* **11,** 329–349.

——, P. Dodge, and M. L. Black, 1991: The landfall of Hurricane Hugo in the Carolinas: Surface wind distribution. *Wea. Forecasting,* **6,** 379–399.

——, S. H. Houston, and I. Ares, 1995: Real-time damage assessment in hurricanes. *Proc. 21st Conf. on Hurricanes and Tropical Meteorology,* Miami, FL, Amer. Meteor. Soc., 500–502.

——, ——, and T. A. Reinhold, 1996: Hurricane Andrew's landfall in South Florida. Part I: Standardizing measurements for documentation of surface wind fields. *Wea. Forecasting,* **11,** 304–328.

Roux, F., and F. D. Marks, 1996: Extended velocity track display (EVTD): An improved processing method for Doppler radar observation of tropical cyclones. *J. Atmos. Oceanic. Technol.,* **13,** 875–899.

SethuRaman, S., 1979: Atmospheric turbulence and storm surge due to Hurricane Belle (1976). *Mon. Wea. Rev.,* **107,** 314–321.

Shapiro, L. J., 1983: The asymmetric boundary layer flow under a translating hurricane. *J. Atmos. Sci.,* **40,** 1984–1998.

Tuleya, R. E., 1994: Tropical storm development and decay: Sensitivity to surface boundary conditions. *Mon. Wea. Rev.,* **122,** 291–304.

——, and Y. Kurihara, 1978: A numerical simulation of the landfall of tropical cyclones. *J. Atmos. Sci.,* **35,** 242–257.

——, M. A. Bender, and Y. Kurihara, 1984: A simulation study of the landfall of tropical cyclones using a movable nested-mesh model. *Mon. Wea. Rev.,* **112,** 124–136.

Wakimoto, R. M., and P. G. Black, 1994: Damage survey of Hurricane Andrew and its relationship to the eyewall. *Bull. Amer. Meteor. Soc.,* **75,** 189–200.

Wang, Y., and G. J. Holland, 1997: On the boundary layer structure under a translating tropical cyclone. Preprints, *22d Conf. on Hurricanes and Tropical Meteorology,* Fort Collins, CO, Amer. Meteor. Soc., 403–404.

Willoughby, H. E., and P. G. Black, 1996: Hurricane Andrew in Florida: Dynamics of a disaster. *Bull. Amer. Meteor. Soc.,* **77,** 543–549.

Wu, J., 1982: Wind-stress coefficients over sea surface from breeze to hurricane. *J. Geophys. Res.,* **87,** 9704–9706.

Zhang, D.-L., Y. Liu, and M. K. Yau, 1999: Surface winds at landfall of Hurricane Andrew (1992)—A reply. *Mon. Wea. Rev.,* **127,** 1711–1721.